Diamond & Related Materials 17 (2008) 1029–1034

Contents lists available at ScienceDirect

Diamond & Related Materials

journal homepage: www.elsevier.com/locate/diamond

Comparative electron diffraction study of the diamond nucleation layer on Ir(001)

S. Gsell [a], S. Berner [b], T. Brugger [b], M. Schreck [a,*], R. Brescia [a], M. Fischer [a], T. Greber [b], J. Osterwalder [b], B. Stritzker [a]

[a] Universität Augsburg, Institut für Physik, D-86135 Augsburg, Germany
[b] Universität Zürich, Physik-Institut, CH-8057 Zürich, Switzerland

ARTICLE INFO

Available online 4 March 2008

Keywords:
Diamond growth and characterisation
Heteroepitaxy
Bias enhanced nucleation
Iridium
XPD

ABSTRACT

The carbon layer formed during the bias enhanced nucleation (BEN) procedure on iridium has been studied by different electron diffraction techniques. In reflection high energy electron diffraction (RHEED) and low energy electron diffraction (LEED) the carbon nucleation layer does not give any indication of crystalline diamond even if the presence of domains proves successful nucleation. In contrast, X-ray photoelectron diffraction (XPD) shows a clear C 1s pattern when domains are present after BEN. The anisotropy in the Ir XPD patterns is reduced after BEN while the fine structure is essentially identical compared to a single crystal Ir film. The change in the Ir XPD patterns after BEN can be explained by the carbon layer on top of a crystallographically unmodified Ir film. The loss and change in the fine structure of the C 1s patterns as compared to a single crystal diamond film are discussed in terms of mosaicity and a defective structure of the ordered fraction within the carbon layer. The present results suggest that the real structure of the BEN layer is more complex than a pure composition of small but perfect diamond crystallites embedded in an amorphous matrix.

1. Introduction

More than 50 years after the first successful synthesis of diamond by the high pressure high temperature (HPHT) [1] method, its extensive application in many fields (e.g. electronics) is still impeded by the lack of large-area high-quality material. The alternative chemical vapor deposition (CVD) technique has in principle the potential to synthesize this type of material. One concept to realize large-area samples by CVD consists in the enlargement of HPHT crystals by homoepitaxial growth [2,3]. The other concept is based on heteroepitaxial deposition of diamond on foreign substrates [4]. This approach, however, requires an appropriate substrate material and an efficient nucleation method. The latter is available since the bias enhanced nucleation (BEN) process has been introduced [5]. With iridium Ohtsuka et al. [6] found a material which provides an ideal substrate for heteroepitaxial diamond deposition ten years ago.

On iridium the diamond grains exhibit an unmatched degree of initial alignment together with an extraordinarily high density [7] which resulted in the first successful deposition of single crystal diamond films via heteroepitaxy [8]. In recent publications it was shown that single crystal iridium films can be integrated on silicon substrates via oxide buffer layers [9]. Thick adhering diamond films with excellent crystal quality were achieved on these substrates of high technological relevance [10,11].

Despite extensive studies [12–14], the mechanisms of BEN on iridium are still not fully understood. After successful diamond nucleation we observe a characteristic pattern formation, i.e. the epitaxial diamond nuclei are gathered in specific areas, which we called “domains” [15]. In a recent X-ray absorption study it was shown that a large fraction of the carbon atoms within these domains reside in a diamond structure, but a reliable quantification was not possible with this technique [16].

Kono et al. first analyzed the Ir surface after BEN by photoelectron diffraction [12]. The modulation amplitude in azimuthal scans was used to determine the fraction of carbon bound in crystalline diamond structure. In addition the authors carefully correlated the deduced anisotropy values for the BEN layers with the morphology of diamond grains grown out of them in a subsequent growth step [17].

In the present work we first examined the long-range order on the Ir surface before and after BEN by reflection high energy electron diffraction (RHEED) and low energy electron diffraction (LEED). The amount of deposited carbon was then determined by X-ray photoelectron spectroscopy (XPS). The main focus of this study was on the acquisition of photoelectron diffraction (XPD) patterns of BEN samples with and without successful diamond nucleation. Since full 3D patterns were measured the analysis of their fine structure allowed us to get deeper insight into the internal structure of the diamond nucleation layer.

* Corresponding author. Tel.: +49 821 598 3401; fax: +49 821 598 3425.
E-mail address: matthias.schreck@physik.uni-augsburg.de (M. Schreck).

0925-9635/$ – see front matter © 2008 Elsevier B.V. All rights reserved.
doi:10.1016/j.diamond.2008.02.040

2. Experimental

Single crystal iridium films with a thickness of 150 nm were deposited on $SrTiO_3$(001) single crystals (10×10×1 mm^3) by e-beam evaporation. Detailed process conditions are described in Ref. [18]. The mosaic spread of the Ir films was in the range between 0.2° and 0.3°, as measured by X-ray diffraction (XRD).

For the bias enhanced nucleation of diamond a microwave plasma chemical vapor deposition (MPCVD) setup was used. It consists of a stainless steel chamber with an inductively heated substrate holder. The BEN step was performed for 45 min at a temperature of about 800 °C, a gas pressure of 30 mbar and a microwave power of 1100 W using a process gas mixture with 7% CH_4 in H_2. The bias voltage of about 280 V was applied to a circular anode while the sample holder was at ground potential [7]. A diamond reference sample with a thickness of 13 μm was grown for 30 h at a reduced methane concentration of 1%, at identical temperature, pressure and microwave power without applied bias voltage. Its mosaic spread was below 0.8°, as determined by XRD.

All the samples were characterised ex-situ. The surface was first imaged by scanning electron microscopy (SEM) using a LEO DSM 982 Gemini instrument.

The crystalline order of the nucleation layer was then studied by RHEED and LEED. RHEED patterns were taken at an electron energy of 30 keV in a separate high vacuum chamber with a base pressure of $2*10^{-8}$ mbar.

The LEED, XPS and XPD experiments were performed in a modified VG ESCALAB 220 photoemission spectrometer with a base pressure in the low 10^{-10} mbar region [19]. The MgK_α source (1253.6 eV) of a twin anode was used for the photoemission experiments. The samples were fixed on a goniometric manipulator, which is capable of polar ($0°<\theta<90°$) and azimuthal ($0°<\phi<360°$) motions. The XPD patterns were obtained by rotation of the sample and recording more than 4000 data points in the upper hemisphere above the surface [20]. The data are stereographically projected on a plane and represented in grey scale, with maximum and minimum intensities as white and black, respectively. The diffraction patterns presented are four fold averaged using the intrinsic symmetry of the surfaces (except for the C 1s pattern of BEN sample A). The coverage of the carbon layers was calculated using standard photoelectron cross sections [21]. A linear background subtraction was applied to determine the intensities of the C 1s and Ir $4d_{5/2}$ core levels. A value of 1.07 nm was used for the mean free path of the Ir $4d_{5/2}$ core level electrons.

Transmission electron micrographs were acquired using a JEOL field-emission JEM-2100F instrument operated at 200 kV.

3. Results

The present study was focused on two BEN samples “A” and “B”. Although both were processed under essentially identical BEN conditions, they showed completely different results in terms of nucleation density. This behaviour is due to the fact that minimum differences in the local ion bombardment conditions can determine whether diamond nucleation takes place or not [14]. Besides the two BEN samples, a pure iridium layer and a heteroepitaxial diamond film served as reference samples for the evaluation of the data.

Fig. 1a shows an SEM micrograph of the Ir reference sample (150 nm Ir on $SrTiO_3$(001)) directly after metal deposition. The surface is dominated by large terraces with only a few small pits. The smoothness becomes also manifest in a streaky RHEED pattern of the

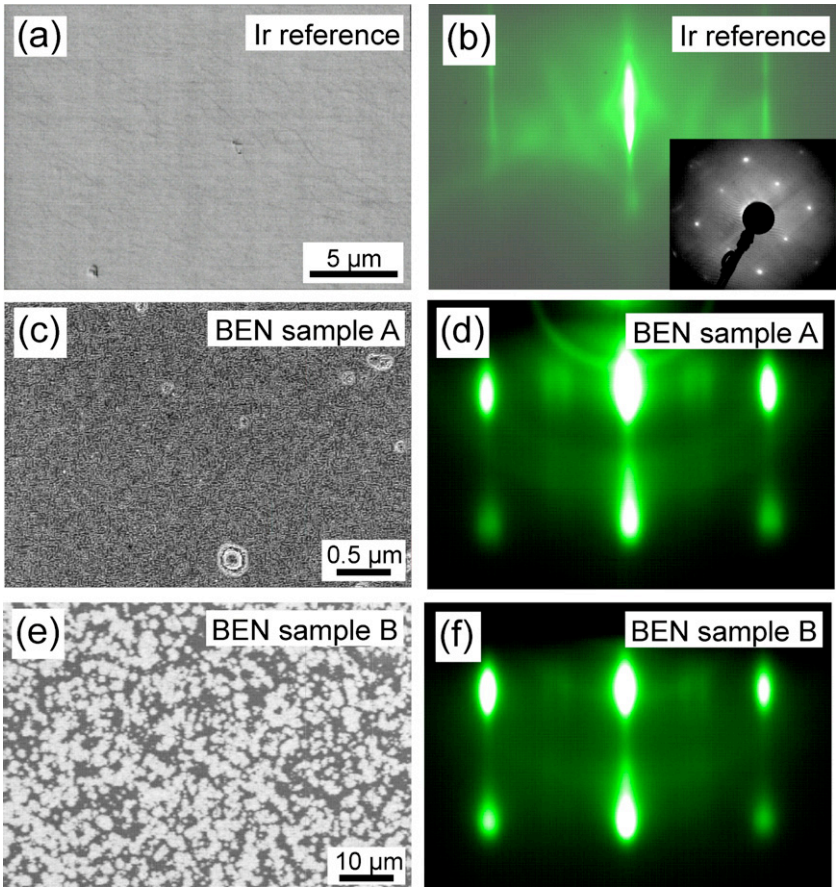

Fig. 1. SEM micrographs (IL detector) and RHEED/LEED patterns of (a), (b) the Ir reference sample, (c), (d) BEN sample A and (e), (f) BEN sample B. In the SEM images the edges are parallel to Ir<110>. The RHEED patterns were taken along Ir<100>.

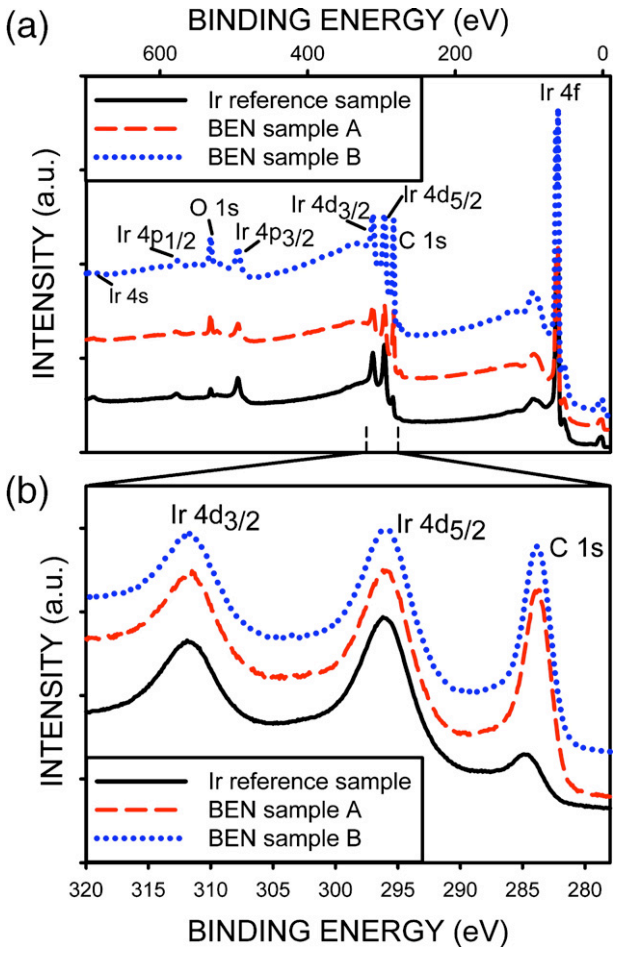

Fig. 2. (a) Wide energy range XPS spectra for the Ir reference sample and the two BEN samples. (b) Detailed view of the Ir 4d and C 1s core levels. The spectra are shifted for better visibility.

Ir 2D surface lattice (Fig. 1b). Furthermore, the clear LEED pattern corroborates the excellent crystalline quality of this epitaxial Ir film.

After diamond nucleation in the MPCVD setup the surface of the BEN sample A in Fig. 1c shows the typical roughening with 2–3 nm deep grooves which are aligned parallel to Ir<110> [22,23]. In former studies it was shown that the diamond nuclei are gathered in the domains which exhibit a bright contrast in SEM micrographs recorded with an annular in-lens (IL) detector [15]. These domains are completely absent on BEN sample A, which clearly indicates that diamond nucleation has not taken place. The corresponding RHEED pattern is dominated by iridium bulk spots and proves that the long-range order in the Ir lattice at the surface is still preserved (Fig. 1d). Furthermore one can identify a splitting of the forbidden Ir(001) reflections. This feature is observed for several roughened samples after BEN on different substrates (Ir/$SrTiO_3$(001) and Ir/YSZ/Si(001)) and is most likely related to the grooved topography. LEED measurements taken for the same sample did not yield a pattern for any electron energy which was varied between 60 and 250 eV.

In contrast to sample A, the SEM micrograph in Fig. 1e of BEN sample B shows a high coverage (~65%) with domains, which proves a successful diamond nucleation. In micrographs with higher magnification (not shown here) one can identify a similar grooved roughening. Likewise the RHEED pattern in Fig. 1f is basically identical to that of BEN sample A. Only spots from a 3D Ir lattice are observed with somewhat weaker intensity of the split Ir(001) reflections. Surprisingly, no diamond-related spots could be identified. Again no reflections at all were obtained in LEED measurements.

Fig. 2a shows wide energy range XPS spectra of all three samples excited by Mg K_α radiation. Besides carbon- and iridium-related maxima one observes small oxygen contaminants due to storage at ambient conditions. From the magnified XPS spectra in chart (Fig. 2b) the positions of the maxima were deduced. All the Ir $4d_{5/2}$ lines are located at a binding energy of 295.9 eV within 0.1 eV. The C 1s XPS peak for the Ir reference is found at 284.4 eV. For both BEN samples the C 1s binding energy of 283.8 eV is consistently lower by 0.6 eV. Thus, in spite of the completely different density of diamond nucleation centers on the two BEN samples there is no measurable difference in the energetic position of the corresponding carbon core level peaks.

Table 1
Carbon coverage data deduced from XPS and anisotropy values extracted from the XPD raw data (after a linear background subtraction) for all the samples studied in this work

	RHEED	LEED	C-coverage (ML) (XPS)	XPD anisotropy Ir 4f | C 1s
Ir reference sample	Ir 2D pattern	Ir pattern	4.3	43% | –
BEN sample A	Ir 3D pattern	No pattern	10.8	33% | 0%
BEN sample B	Ir 3D pattern	No pattern	10.8	31% | 12%
BEN sample B+1 h at 520 °C	–	–	10.1	31% | 13%
BEN sample B+1 h at 520 °C +0.5 h at 800 °C	–	–	10.3	30% | 12%
Diamond reference sample	–	–	–	– | 67%

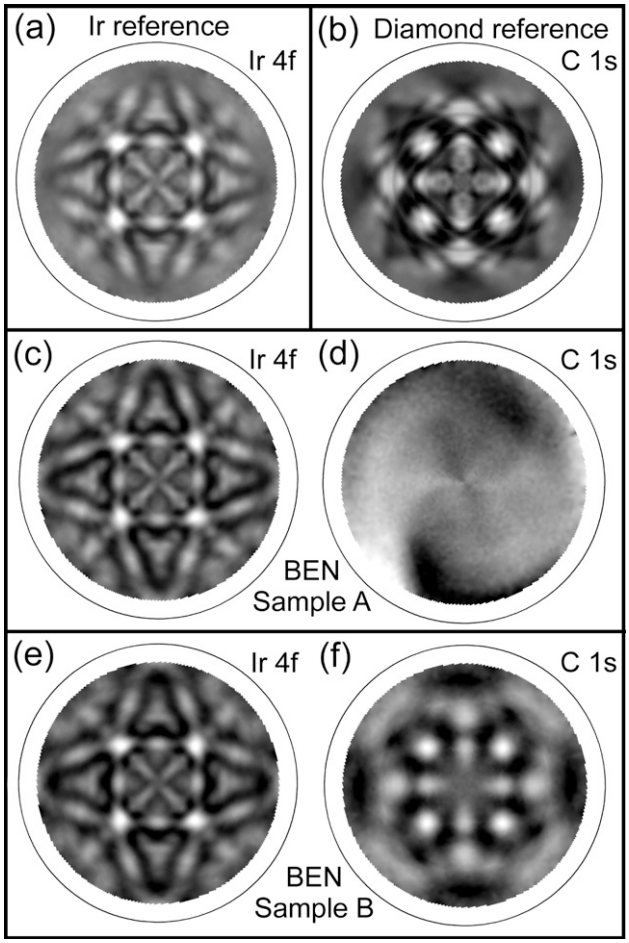

Fig. 3. XPD patterns of the Ir 4f and the C 1s core levels for (a) the Ir reference and (b) the diamond reference sample as well as for (c), (d) BEN sample A and (e), (f) BEN sample B.

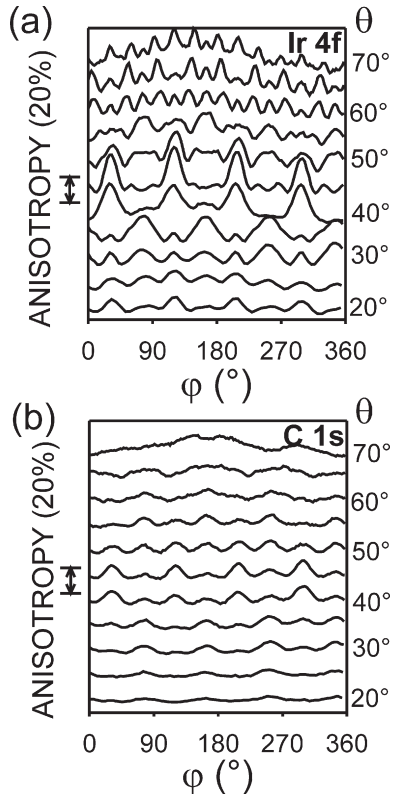

Fig. 4. Azimuthal scans over a range of 0–360° extracted from XPD patterns for (a) Ir 4f and (b) C 1s photoemission lines measured on BEN sample B (raw data without 4-fold averaging).

From the integral intensities a quantitative analysis of the carbon coverage was performed by assuming a homogeneous carbon layer on top of the iridium substrate. The values are summarized in Table 1. The carbon coverage amounts to 4.3 ML on the Ir reference sample and to 10.8 ML on the BEN samples A and B. Here, 1 ML (monolayer) is defined as the area density of carbon atoms equivalent to a quarter of a diamond lattice cell (a_0=0.356 nm, 1 ML=0.089 nm, 1 ML=1.58·10^{15} C-atoms/cm^2).

Photoelectron diffractograms of the Ir 4f XPS peak for the Ir reference and the two BEN samples are presented in Fig. 3a, c and e respectively. All patterns exhibit a clear 4-fold symmetry in accordance with an Ir(001) surface. Significant differences between the Ir 4f diffractograms for BEN samples A and B are not detectable. The fine structure of the latter two XPD patterns is not affected by the higher coverage with carbon as compared to the one of the Ir reference sample.

In contrast, the C 1s XPD diffractograms of the two BEN samples in chart 3d and 3f differ dramatically. For BEN sample A (no domain formation) a nearly homogeneous background intensity is obtained. The residual contrast with seemingly twofold symmetry represents an artifact. It originates from the rectangular size of the sample (5×10 mm^2) which results in a variation of the analyzed area when the sample is rotated during the measurement. For BEN sample B with the high coverage of domains a clear C 1s XPD pattern (Fig. 3f) with 4-fold symmetry is measured. In chart 3b the C 1s XPD pattern of the diamond single crystal reference sample is shown for comparison. The overall structure is similar but the fine structure differs significantly between the two diffractograms. This indicates that a high fraction of carbon atoms at the surface of BEN sample B is arranged in a crystalline diamond structure.

Fig. 4 shows full azimuthal scans at fixed polar angles θ for the BEN sample B which were extracted from the corresponding Ir 4f and C 1s XPD diffractograms in Fig. 3e and f. The ordinate, the so called anisotropy, is defined as $(I-I_a)/I_a$, where I is the intensity at the azimuthal angle ϕ and I_a is the average over the whole azimuthal range at the corresponding fixed polar angle. The C 1s and the Ir 4f patterns exhibit maximum anisotropies of 12% and 31%, respectively. The maxima in intensity are at a polar angle of about 45° along the four <101> directions. For these directions the nearest-neighbor distance is the smallest and the forward scattering the strongest.

The anisotropy value of the Ir 4f signal for the two BEN samples A and B is nearly identical (33% for A and 31% for B) which has to be compared with the 43% measured for the Ir reference sample (see Table 1). A similar comparison considering the carbon signals yields 0% and 12% for samples A and B, respectively, and 67% for the diamond reference sample.

In order to obtain further input for a detailed interpretation of these findings we also studied the thermal stability of the structures that cause the anisotropy. In a first experiment the BEN sample B was annealed for 1 h at a temperature of 520 °C in the combined XPS/XPD analysis chamber. Fig. 5a shows the corresponding XPS spectra in the region of the C 1s and Ir 4d peaks. After this annealing procedure one observes a slight reduction in the peak intensity of the C 1s signal which corresponds to a decrease of the carbon coverage by 0.7 ML to a value of 10.1 ML (see Table 1). In Fig. 5b azimuthal scans for the C 1s core level are shown at a polar angle of about 45° where the maximum anisotropy is observed. For BEN sample B after the first annealing

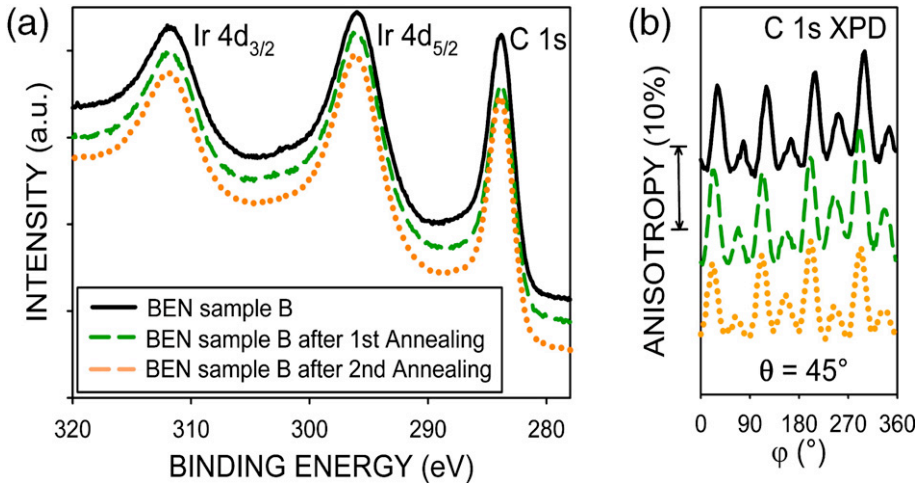

Fig. 5. (a) XPS spectra in the region of the Ir 4d and C 1s XPS peaks for BEN sample B before and after the first (520 °C/1 h) and the second (800 °C/0.5 h) annealing step in ultra high vacuum. (b) Corresponding XPD azimuthal scans of the C 1s core level at a polar angle of about 45°. The legend is common to both charts.

treatment the anisotropy for the C 1s and the Ir 4f (not shown) is almost unchanged (Table 1).

In a second annealing step a temperature of 800 °C, which is similar to the conditions during BEN, was applied for 0.5 h. The carbon coverage of 10.3 ML remained nearly constant as compared to the coverage after the first annealing step; the small deviation of 0.2 ML is within the experimental error of measurement setup and data evaluation. The anisotropy deduced from azimuthal scans of the C 1s (Fig. 5b) and Ir 4f patterns (not shown) after this second annealing step is nearly unaltered. We therefore conclude that the crystalline carbon structures which cause the diamond XPD pattern are stable at 800 °C even without the ion bombardment and plasma environment which is present during the BEN process.

4. Discussion

In former studies on heteroepitaxial diamond nucleation Kono et al. examined the Ir surface by LEED and XPD after different BEN processes which were performed in a three-electrode [12], in a planar-diode [17] DC-plasma system and in a microwave plasma setup [13]. To determine the forward scattering patterns the authors measured azimuthal scans over an angular range 0–180° at polar angle distances of 5°. From the maxima and minima they deduced anisotropy values for the XPD patterns of the Ir 4d and the C 1s core levels. They interpreted the anisotropy values determined for the BEN samples as compared to single crystal Ir in terms of a loss of crystalline order for iridium. Furthermore they deduced the volume fraction of crystalline diamond islands embedded in an amorphous carbon matrix from the anisotropy of the C 1s signal compared to that of a diamond reference sample.

In the present study full XPD patterns were measured over an angular range of ϕ=0–360° and θ=0–80°. It turned out immediately that the diffractograms contain plenty of fine structure which can yield additional information. All Ir patterns show a similar fine structure while in the carbon pattern of the BEN layer fine details are lost as compared to the single crystal diamond film. At the same time the anisotropy values have decreased in both cases.

Apparently neither the roughening of the surface after BEN accompanied by the formation of side facets nor the carbon layer on top have a pronounced effect on the fine structure of the Ir patterns. We attribute the decrease in anisotropy as compared to the Ir single crystal film for both BEN samples primarily to the presence of the carbon layer deposited during BEN.

Several independent methods have indicated that it is a continuous closed carbon film with a high electrical resistivity. Outside the domains its structure is purely amorphous while inside the domains diamond nuclei are embedded [14,16]. A closed layer structure is an imperative precondition for a reasonable evaluation of film thicknesses from XPS peak intensities. The 0.96 nm determined in the present study fit well the ~1 nm determined in former publications by elastic recoil detection analysis [24] and TEM [25]. Since former TEM work was done on BEN samples with high domain density we independently checked the film thickness for sample A (no domain formation) by TEM in this study. Fig. 6 shows a cross section TEM micrograph of BEN sample A which was covered by an additional 10-nm-thick Ir top layer after BEN in order to enhance the contrast and protect the carbon film [25]. Similar to the former TEM studies a bright slit due to the BEN layer is visible, which exhibits a thickness of 1–2 nm. Therefore we conclude that this precursor phase is always deposited at typical BEN conditions. Its formation is a necessary but not sufficient condition that diamond nucleation really occurs. The latter requires a careful fine tuning of the local ion bombardment conditions.

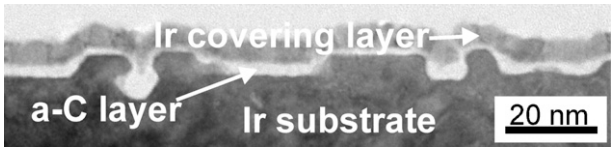

Fig. 6. Cross section TEM image of BEN sample A.

The carbon layer deposited during BEN suppresses any LEED pattern. This can be easily understood taking into account the inelastic mean free path of below 1 nm for electrons with kinetic energies of 50–300 eV typical for LEED [26]. For the 30 keV RHEED electrons the mean free path is high enough (>4 nm [27]) especially since the roughening allows 3D scattering. In the XPD patterns the overlayer apparently does not destroy the fine structures. Instead of this, it increases the isotropic part of the Ir XPS signal due to scattering events within the carbon film. In this way it reduces the anisotropy.

The carbon layer does not give any signal in LEED and RHEED for both BEN samples. One can therefore directly exclude that the bright domains which cover 65% of the surface of sample B represent areas of single crystal diamond. The two electron diffraction methods rely on the interference of many partial waves stemming from cells of extended crystallites, i.e. these methods require a long-range order. The absence of carbon-related patterns indicates a low crystalline order due to very small crystallites and/or highly defective structures. While the LEED results could also be consistent with a crystalline diamond layer covered by an amorphous overlayer the absence of the RHEED patterns argues against this possibility.

In contrast to LEED and RHEED, XPD shows clear patterns for the domain sample B, which substantiates that carbon atoms reside in a diamond structure within the domains. However, the fine structure is much less pronounced compared with the pattern of the hetero-epitaxial diamond film on Ir/YSZ/Si(001). The latter yields an excellent single crystal reference since it is nearly identical to the pattern of a diamond single crystal reported in literature [28].

As a first explanation for the fine structure of the carbon XPD pattern deviating from its single crystal reference one may consider the finite thickness of the BEN layer. Actually, simulations of diamond XPD patterns for different thicknesses reported in literature show a strong variation especially within the first 5 ML [29]. However, we could not find a satisfying correspondence with our measured patterns.

In contrast, the fine structure of the present C 1s pattern shows a striking similarity to the XPD pattern taken by Schaller et al. [28] from highly oriented diamond films heteroepitaxially grown on silicon. Layers of this type and thickness typically show a mosaic spread of 5–10°. Since a highly defective crystal structure can be ruled out as an explanation, the blurring in their pattern has to be attributed to the angular spread in crystallite orientation.

From this observation we directly conclude that a data evaluation which considers only two components – a completely amorphous phase and a perfectly aligned and crystalline diamond phase – may not be adequate to interpret the data completely.

Kono et al. reported anisotropy values of 46%, 26% and 22% for the C 1s signal of the different BEN samples in their studies [12,13,17]. In the present study we measure a value of 12%. Taking into account the domain coverage of 65% for BEN sample B we obtain a maximum value of ~18%. Comparing this with 67% as determined for our diamond reference sample we conclude that at least one fourth of the carbon atoms within the domains reside in a crystalline diamond environment. The present estimation can only give a lower limit since blurring in the fine structure is supposed to decrease anisotropy values.

Attributing the measured anisotropy and the blurring exclusively to an angular spread of small diamond grains embedded in an amorphous carbon matrix one would expect to find a large number of extended diamond crystallites. With a typical distance of 25 nm (corresponding to a nucleation density of 1.6×10^{11} cm^{-2}) these should have a lateral size of ~13 nm. In several TEM studies of BEN samples the search for crystalline diamond structures has always been

unsuccessful [25]. Even after 5 s growth diamond crystallites have not yet reached this lateral extension [30]. In addition, 13-nm large crystals should give some signal in RHEED. We therefore propose a refined model for the structure of the diamond nucleation layer which postulates the existence of three different phases. Outside the domains there is a completely amorphous carbon layer. Within the domains a large fraction of the carbon atoms resides in a highly defective crystalline structure which can not be seen in TEM or by RHEED. However they yield the dominant contribution to the XPD pattern. Extremely small crystallites not detectable by HRTEM are embedded in this matrix which represent the nuclei that survive after termination of the BEN treatment and switching to standard growth conditions. In addition some amorphous carbon may also be present.

From the annealing experiments we draw the conclusion that all three phases are stable under heat treatment at 800 °C. This information is especially important for the defective crystalline structure that does not decompose and desorb at these temperatures.

5. Summary

In RHEED and LEED the carbon layer formed by BEN does not give any indication of crystalline diamond even if the presence of domains proves the successful nucleation process. In contrast, XPD measurements yield a clear C 1s pattern for samples which show domains after BEN. The anisotropy in the Ir XPD patterns is reduced by the biasing procedure while its fine structure is essentially unchanged. This can be explained by the presence of a carbon BEN layer on top of a usually roughened but crystallographically unmodified Ir layer. The loss and change in fine structure of the C 1s XPD pattern originating from the BEN sample with domains as compared to a single crystal diamond film can result from a certain mosaic spread and a high level of defects in the ordered regions of the carbon layer. It is suggested that besides amorphous carbon and tiny diamond crystallites that represent the nuclei, a third phase of ordered carbon is present. It yields the main contribution to the carbon XPD pattern and it can be described as a highly defective oriented diamond structure.

References

[1] F.P. Bundy, H.T. Hall, H.M. Strong, R.H. Wentorf, Nature 176 (1955) 51.
[2] Y. Mokuno, A. Chayahara, Y. Soda, Y. Horino, N. Fujimori, Diamond Relat. Mater. 14 (2005) 1743.
[3] S.S. Ho, C.S. Yan, Z. Liu, H.K. Mao, R.J. Hemley, Ind. Diamond Rev. 1 (2006) 28; C.-S. Yan, Y.K. Vohra, H.-K. Mao, R.J. Hemley, Proc. Natl. Acad. Sci. U. S. A. 99 (2002) 12523.
[4] ST. Lee, Y. Lifshitz, Nature 424 (2003) 6948.
[5] S. Yugo, T. Kanai, T. Kimura, T. Muto, Appl. Phys. Lett. 58 (1991) 1036.
[6] K. Ohtsuka, K. Suzuki, A. Sawabe, T. Inuzuka, Jpn. J. Appl. Phys. 35 (1996) L1072.
[7] M. Schreck, H. Roll, B. Stritzker, Appl. Phys. Lett. 74 (1999) 650.
[8] M. Schreck, F. Hörmann, H. Roll, J.K.N. Lindner, B. Stritzker, Appl. Phys. Lett. 78 (2001) 192.
[9] S. Gsell, M. Fischer, R. Brescia, M. Schreck, P. Huber, F. Bayer, B. Stritzker, D.G. Schlom, Appl. Phys. Lett. 91 (2007) 061501.
[10] S. Gsell, T. Bauer, J. Goldfuß, M. Schreck, B. Stritzker, Appl. Phys. Lett. 84 (2004) 4541.
[11] T. Bauer, S. Gsell, M. Schreck, J. Goldfuß, J. Lettieri, D.G. Schlom, B. Stritzker, Diamond Relat. Mater. 14 (2005) 314.
[12] S. Kono, T. Takano, T. Goto, Y. Ikejima, M. Shiraishi, T. Abukawa, T. Yamada, A. Sawabe, Diamond Relat. Mater. 13 (2004) 2081.
[13] S. Kono, M. Shiraishi, N.I. Plusnin, T. Goto, Y. Ikejima, T. Abukawa, M. Shimomura, Z. Dai, C. Bednarski-Meinke, B. Golding, New Diam. Front. Carbon Technol. 15 (2005) 363.
[14] S. Gsell, M. Schreck, G. Benstetter, E. Lodermeier, B. Stritzker, Diamond Relat. Mater. 16 (2007) 665.
[15] M. Schreck, Th. Bauer, S. Gsell, F. Hörmann, H. Bielefeldt, B. Stritzker, Diamond Relat. Mater. 12 (2003) 262.
[16] P. Bernhard, C. Ziethen, G. Schoenhense, M. Schreck, T. Bauer, S. Gsell, B. Stritzker, Jpn. J. Appl. Phys. 45 (2006) L984.
[17] T. Aoyama, N. Amano, T. Goto, T. Abukawa, S. Kono, Y. Ando, A. Sawabe, Diamond Relat. Mater. 16 (2007) 594.
[18] F. Hörmann, H. Roll, M. Schreck, B. Stritzker, Diamond Relat. Mater. 9 (2000) 256.
[19] T. Greber, O. Raetzo, T.J. Kreutz, P. Schwaller, W. Deichmann, E. Wetli, J. Osterwalder, Rev. Sci. Instrum. 68 (1997) 4549.
[20] J. Osterwalder, T. Greber, A. Stuck, L. Schlapbach, Phys. Rev. B 44 (1991) 13764.
[21] J.J. Yeh, I. Lindau, At. Nucl. Data Tables 32 (1985) 1–155.
[22] Th. Bauer, S. Gsell, F. Hörmann, M. Schreck, B. Stritzker, Diamond Relat. Mater. 13 (2004) 335.
[23] F. Hörmann, M. Schreck, B. Stritzker, Diamond Relat. Mater. 10 (2001) 1617.
[24] Th. Bauer, M. Schreck, F. Hörmann, A. Bergmaier, G. Dollinger, B. Stritzker, Diamond Relat. Mater. 11 (2002) 493.
[25] M. Schreck, F. Hörmann, S. Gsell, Th. Bauer, B. Stritzker, Diamond Relat. Mater. 15 (2006) 460.
[26] M.P. Seah, W.A. Dench, Surf. Interface Anal. 1 (1979) 2.
[27] M. Desjonqueres, D. Spanjaard, Concepts in Surface Physics, Springer Series in Surface Sciences, vol. 30, 1993.
[28] E. Schaller, O.M. Küttel, P. Aebl, L. Schlapbach, Appl. Phys. Lett. 67 (1995) 1533.
[29] E. Maillard-Schaller, O.M. Kuettel, L. Schlapbach, Phys. Status Solidi A 153 (1996) 415.
[30] R. Brescia, S. Gsell, M. Fischer, M. Schreck, B. Stritzker, Diamond Relat. Mater. (in press).